Buoyancy Effect of Unsteady Magnetohydrodynamic Thermal Transportation of TiO_2-Kerosene Nanofluids within a Wavy Octagonal Domain including Heated Rectangular Vertical Wall

Tinni Saha*

Abstract: In this paper, modeling of mathematics of MHD two dimensional unsteady flow of natural convection and transportation of heat inside a wavy octagonal enclosure including Rectangular vertical wall (RVW) which is fill up by TiO2-Kerosene nanofluids is investigated. The RVW is hot with temperature $T = T_h$ while the wavy wall is cold with temperature $T = T_c$ where $T_c<T_h$. All other boundary of the domain is assumed adiabatic. In numerical simulation, the Galerkin type finite element method, the solver of influential partial differential equations, has been occupied here. A wonderful agreement is seen here to compare the result with the previously published research paper. About 0.68 dimensionless time is taken to the heat transport process of the numerical solution's to reach from unsteady situation to a steady-state. For the variety of the pertinent parameter *Ra*, the Rayleigh number *i.e.* buoyancy force effect on local and mean Nusselt number, streamlines and isotherms are displayed here. Heat transportation rate enhances for growing up of buoyancy force.

Keywords: Unsteady flow, MHD, Nanofluids, Wavy wall, Octagonal shape domain.

Introduction

Within various enclosures free convective flow of fluid and transfer of heat of MHD flow has been reached on a remarkable consideration for its direct applications on engineering like geophysical fluid mechanics, solar engineering applications, cooling of nuclear reactor, fire engineering, electrical systems, enlarging the systems of cooling in the vehicle, petroleum reservoirs exchangers of heat etc. Less noise, simplicity, and lower cost are the main superiority of free convective cooling systems. Al-weheibi *et al.* [1] researched numerically natural convective thermal transfer in a enclosure

*Tinni Saha, Assistant Professor, OSD, Ministry of Education & former student, Department of Mathematics, Eden Mohila College, Dhaka.

shaped trapezoid which is fill up with nanoparticles. Balushi *et al.* [2] investigated free convective thermal transfer utilizing magnetic nanoparticles in a square enclosure. Enhancing thermal conductivity of fluids was enhanced by Choi and Eastman [3] with nanoparticles. Dogonchi *et al.* [4] analyzed numerically natural convection on triangular shape cavity with semicircular bottom wall fill up with Cu–water nanofluid. Natural convective flow in influence of a magnetic field performed by Ece and Buyuk [5], in an inclined domain of rectangular shaped cooled and warmed on adjacent partition. In a square shaped domain fill up with nanofluid, magnetic fields' effects on natural convection were done by Ghasemi *et al.* [6]. In a domain of rectangular shape, buoyancy-driven thermal transfer of water-based Al_2O_3 nanofluids was presented by Hwang *et al.* [8]. Jang and Choi [9] were taken Brownian motion to see its role in the nanofluids' greater thermal conductivity. A square shape inclined enclosure in nanofluids was used by Kalbani and Rahman [10] to observe convective heat transfer in the company of intend magnetic field and heat source Brownian motion.

MHD mixed convective thermal transfer having vertical fin in a lid-driven square domain was investigated numerically by Md-Fayz *et al.* [11]. Nasrin and parvin [12] investigated transportation of heat and buoyancy-operated flow in trapezoidal cavity which was filling up with nanofluid water-Cu. Natural convection in rectangle shape enclosures which is heated partially fill up with nanofluids was examined by Oztop and Abu-Nada [13]. Parvin and Nasrin [14] observed Effects of Prandtl and Reynolds number on mixed convection with a heat-generating hollow cylinder in an octagonal channel. Unsteady MHD convection in a semi-circular domain which was filled with ferrofluid analyzed numerically and statistically by Rahman *et al.* [15].

Free convective heat transport within octagonal domain analyzed by Saha *et al.* [16]. Thermal influences of heated fin inside a wavy square cavity on MHD natural convective flow of nanofluids were examined by Tinni *et al.* [17]. Computational procedure of finite element was computed by Uddin *et al.* [18] in an annulus, for convective flow of nanofluids. Wong and Leon [19] reviewed current and upcoming applications of nanofluids. The research gap noticed in literature of this study including:

- No study has been done on unsteady, fluid flow and thermal transfer from heated RVW on wavy octagonal cavity.
- Lacking of enough details covering the nanoparticles shapes' effect.

- Lacking of sufficient experimental particulars of nanofluids, in spite of its extensive thermophysical properties.
- The shape of octagonal cavity has gained some attention, but further research is required to ascertain which geometry will greatest facilitate thermal transfer.

To investigate the free convective unsteady heat transport and flow of nanofluids in wavy octagonal domain including RVW under magnetic fields' influence is the main aim of this numeric analysis. Taking into consideration the significance of nanofluids thermal performance with effects of magnet in various processes of engineering including decomposition of silver, exchanger of heat, crystallization, evaporation of water, etc.

Modeling of Physics

A two-dimensional incompressible, dependent on time, laminar, naturally convective heat transportation and flow of nanofluids in an octagonal domain with wavy top borderline and hot RVW on the middle of the bottom wall under the influence of magnetic field considered as mathematical model. *x*-axis, the dimensional coordinate plan through the base partition and *y*-axis is normal to *x*-axis. The boundaries of cavity assumed fixed. Free convection introduced by build differences of temperature among warmed RVW on centre of the bottomed wall and wavy top cool walls. The warmed RVW on the foundation wall is uniformly heated at T_h temperature, though the wavy top boundary is cold at low temperature T_c ($T_c < T_h$).

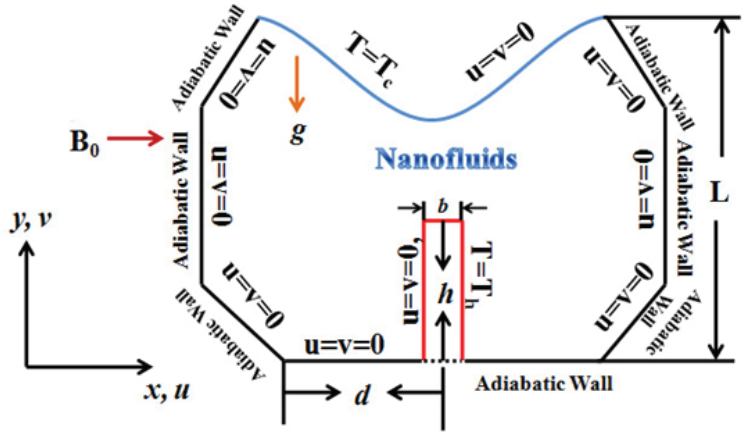

Figure 1: Schematic view of wavy octagonal cavity with RVW and boundary conditions.

It is hint up that into conventional fluid; the particles of nano-sized are distributed homogenously. Between nanoparticles and the conventional fluids, thermal slip and the thermal equilibrium exit. It is also bring up that during convection, between the nanofluids' thermo-physical properties, where another properties are remain fixed, density; the property that is physical in buoyancy term differs. This condition is reasonable since the variety of temperature is limited between hot and cold boundaries. The acceleration cause of gravity works in opposite direction of *y*-axis. All the solid walls are considered as firm no-slip boundaries. Together with systems of coordinate the geometry are graphically depict in Figure 1. Properties of thermo-physics of different conventional fluids and nanoparticles are writing down in Table 1.

Conventional Fluid/ Nanoparticles	c_p [$Jkg^{-1}K^{-1}$]	P [kgm^{-3}]	k [$Wm^{-1}K^{-1}$]	μ [$kgm^{-1}s^{-1}$]	$\beta\times10^{-5}$ [K^{-1}]	σ [Sm^{-1}]	Pr
Kerosene	2090	780	0.149	0.00164	99	6.0×10^{-10}	23.004
TiO_2	686.2	4250	8.9538	-	0.90	2.60×10^{6}	-

Table 1: Properties of thermo-physics of different founded fluid and solid nanoparticles.

Modeling of Mathematics

For the present thesis, to extract the equations that governs in the form of dimensional applying the aforementioned assumption as follows:

Equation of Continuity:

$$\frac{\partial u}{\partial x}+\frac{\partial v}{\partial y}=0 \tag{1}$$

x-directed Momentum equation:

$$\rho_{nf}\left(\frac{\partial u}{\partial t}+u\frac{\partial u}{\partial x}+v\frac{\partial v}{\partial y}\right)=-\frac{\partial p}{\partial x}+\mu_{nf}\left(\frac{\partial^2 u}{\partial x^2}+\frac{\partial^2 u}{\partial y^2}\right) \tag{2}$$

y-directed Momentum equation:

$$\rho_{nf}\left(\frac{\partial v}{\partial t}+u\frac{\partial v}{\partial x}+v\frac{\partial v}{\partial y}\right)=-\frac{\partial p}{\partial y}+\mu_{nf}\left(\frac{\partial^2 v}{\partial x^2}+\frac{\partial^2 v}{\partial y^2}\right)+(\rho\beta)_{nf}\,g(T-T_c)-\sigma_{nf}\,{B_0}^2 v \tag{3}$$

Equation of energy:

$$\frac{\partial T}{\partial t}+u\frac{\partial T}{\partial x}+v\frac{\partial T}{\partial y}=\alpha_{nf}\left(\frac{\partial^2 T}{\partial x^2}+\frac{\partial^2 T}{\partial y^2}\right) \tag{4}$$

where velocity unit through *x, y* coordinates are *u, v,* respectively, the gravity is *g,* the pressure is *p*, temperature is *T*, temperature of reference is T_c, density is ρ_{nf} of nanofluid, dynamic viscosity is μ_{nf} of nanofluid, the thermal diffusivity is $\alpha_{nf} = k_{nf} / (\rho c_p)_{nf}$ of nanofluid, the heat capacity is $(\rho c_p)_{nf}$ of nanofluid, the thermal conductivity is k_{nf} of nanofluid, the volumetric thermal expansion is $(\rho\beta)_{nf}$ of nanofluid.

Initial and Boundary Conditions

The initial and boundary conditions of narrated modeling above are given below:

For t 0; entire domain: $u = 0, v = 0, T = T_c, p = 0$ (5a)

For t 0;

At the Topper wall**:** $x = a\cos 2\pi\lambda_0 x;\ T = T_c, u = 0, v = 0$ (5b)

At the two sides (left and right side) walls: u = v = 0, $\frac{\partial T}{} = 0$ (5c)

At the bottomed wall: u = v = 0, $\frac{\partial T}{} = 0$ (5d)

At inclined walls: u = v = 0, $\frac{\partial T}{} = 0$ (5e)

At the RVW surface: $0 \leq y$ h; x d $\frac{b}{}$ and x d $\frac{b}{}$ (5f)

At the RVW surface: u = v = 0, $T = T_h$ (5g)

The Nanofluids' Thermal and Physical belongings

The nanofluids' physical and thermal characteristics are significant for intensifying the thermal execution of nanofluids. Following thermal and physical belongings of nanofluids are taken under consideration and note down as the density, the viscosity, the electrical conductivity, the heat capacitance, the thermal expansion coefficient, the thermal conductivity and the thermal diffusivity respectively (see Al-Weheibi *et al.* [1], Kalbani *et al.* [10], and Uddin *et al.* [18]):

The nanofluids' effectual viscosity is given bellow:

$$\mu_{nf} = \mu_{bf} \frac{1}{(1-\phi)^{2.5}} \tag{6}$$

when nanoparticles' volume fraction is represented by .

The nanofluids' effective density is indicated as bellow:

$$\rho_{nf} = (1-\phi)\rho_{bf} + \phi\rho_{sp} \tag{7}$$

The nanofluids' thermal diffusivity is demonstrating bellow:

$$\alpha_{nf} = \frac{k_{nf}}{(\rho c_p)_{nf}} \tag{8}$$

The nanofluids' heat capacitance is given by

$$(\rho c_p)_{nf} = (1-\phi)(\rho c_p)_{bf} + \phi(\rho c_p)_{sp} \tag{9}$$

By Hamilton and crosser [13], thermal conductivity's Maxwell model is expanded with a factor of shape as follows:

$$\frac{k_{nf}}{k_{bf}} = \frac{k_{sp} + (n-1)k_{bf} - (n-1)(k_{bf} - k_{sp})\phi}{k_{sp} + (n-1)k_{bf} + (k_{bf} - k_{sp})\phi} \tag{10}$$

The nanofluids' electrical conductivity is expressed by the method

$$\sigma_{nf} = \frac{\sigma_{sp} + 2\sigma_{bf} - 2(\sigma_{bf} - \sigma_{sp})\phi}{\sigma_{sp} + 2\sigma_{bf} + (\sigma_{bf} - \sigma_{sp})\phi}\sigma_{bf} \tag{11}$$

The coefficient of thermal expansion is determined as follows

$$(\rho\beta)_{nf} = (1-\phi)(\rho\beta)_{bf} + \phi(\rho\beta)_{sp} \tag{12}$$

Dimensional Analysis

To transform the governing as well as controlling equations (1)-(4) for the current study, the bellows dimensionless variables are induced including starting and borderlines' conditions (5a) - (5g) into dimensionless form.

$$\begin{aligned} &X = \frac{x}{L}, Y = \frac{y}{L}, U = \frac{uL}{\alpha_{bf}}, V = \frac{vL}{\alpha_{bf}}, \theta = \frac{T - T_c}{T_h - T_c}, P = \frac{pL^2}{\rho_{nf}{\alpha_{bf}}^2}, \\ &\tau = \frac{t\alpha_{bf}}{L^2}, \lambda = \frac{\lambda_0}{L}, D = \frac{d}{L}, H = \frac{h}{L}, A = \frac{a}{L}, B = \frac{b}{L} \end{aligned} \tag{13}$$

Employing equation (13) into (1)-(4) including starting and borderlines' conditions (5a)-(5g) as bellowing

$$\frac{\partial U}{\partial X} + \frac{\partial V}{\partial Y} = 0 \tag{14}$$

$$\frac{\partial U}{\partial \tau} + U\frac{\partial U}{\partial X} + V\frac{\partial U}{\partial Y} = -\frac{\rho_{bf}}{\rho_{nf}}\frac{\partial P}{\partial X} + \Pr\frac{\mu_{nf}}{\mu_{bf}}\frac{\rho_{bf}}{\rho_{nf}}\left(\frac{\partial^2 U}{\partial X^2} + \frac{\partial^2 U}{\partial Y^2}\right) \tag{15}$$

$$\frac{\partial V}{\partial \tau}+U\frac{\partial V}{\partial X}+V\frac{\partial V}{\partial Y}=-\frac{\rho_{bf}}{\rho_{nf}}\frac{\partial P}{\partial Y}+\Pr\frac{\mu_{nf}}{\mu_{bf}}\frac{\rho_{bf}}{\rho_{nf}}\left(\frac{\partial^2 V}{\partial X^2}+\frac{\partial^2 V}{\partial Y^2}\right)+\frac{(\rho\beta)_{nf}}{\rho_{nf}\beta_{bf}}Ra\Pr\theta-\frac{\rho_{bf}}{\rho_{nf}}\frac{\sigma_{nf}}{\sigma_{bf}}Ha^2\Pr V \quad (16)$$

$$\frac{\partial \theta}{\partial \tau}+U\frac{\partial \theta}{\partial X}+V\frac{\partial \theta}{\partial Y}=\frac{\alpha_{nf}}{\alpha_{bf}}\left(\frac{\partial^2 \theta}{\partial X^2}+\frac{\partial^2 \theta}{\partial Y^2}\right) \quad (17)$$

In the over headed dimensionless governing equations, $Ra=\frac{g\beta_{bf}(T_h-T_c)L^3}{\nu_{bf}\alpha_{bf}}$; the Rayleigh number, the Prandtl number is $\Pr=\frac{\nu_{bf}}{\alpha_{bf}}$ and the Hartmann number is $Ha=B_0L\sqrt{\sigma_{bf}/\mu_{bf}}$

The Dimensionless Form of the Boundary Conditions

For = 0, entire domain: P = 0, U = 0, V = 0, = 0 (18a)

For , the dimensionless borderlines' conditions:

At the top wall: θ = 0, U = 0, V = 0 (18b)

At the right and left side boundaries: U = 0, V = 0, ∂θ/∂X=0 (18c)

At the bottomed wall: U = 0, V = 0, ∂θ/∂Y=0 (18d)

At inclined walls: U = 0, V = 0, ∂θ/∂N=0 (18e)

On the RVW surface: 0≤Y≤H; X=D+B/2 and X=D-B/2 . (18f)

At the RVW walls: U = V = 0, θ = 1 (18g)

Nusselt Number Calculation

Average and local Nusselt number at hot RVW are expressed respectively by:

$$Nu_L=\frac{Lq_w}{k_{bf}(T_h-T_c)} \quad \text{Where} \quad q_w=-k_{nf}\left(\frac{\partial T}{\partial y}\right)_{y=0} \quad (19)$$

$$Nu_{av}=\left(\frac{k_{nf}}{k_{bf}}\right)\int\frac{\partial\theta}{\partial Y}dX \quad (20)$$

Computational Process

Galerkin weighted residuals' finite element analysis is applied which formed the dimensionless governing equations. (14)–(17) along with borderline conditions (18a)–(18g) are acted. Zienkiewicz *et al.* [25] widely described the numerical procedures. Making use of the magnificent Comsol Multi physics; the PDEs solver, computation process for this

problem is skilled. By discretizing the domain of the solution, non-uniform triangular components are set up to short grid numbers first. For development of the present technique, there's applied triangular elements of six nodes. After then, utilizing the technique of Galerkin weighted residual, established integral equations from equations of governing PDEs. In each and every part of integral equations, Gauss's quadrature process is also employed. Using borderline conditions these equations are also improvised. Newton–Raphson iteration method is utilized to solve these algebraic equations in the form of matrix. The techniques' convergence norm is tried as $\left|M^{i+1} - M^{i}\right| \leq 10^{-5}$, where M specifies θ, U, V as dependent variables and i is the number of iteration.

Independency Test of Grid

For independent test of grid, for the present problem, a non-uniform comprehensive grid sensitivity is looked at when $Ra = 10^5$, $Ha = 20$, $Pr = 23.004$, $\phi = 0.04$, $n = 3$ and $\tau = 1$ in the wavy octagonal cavity with RVW. Five distinct non-uniform methods of grid which

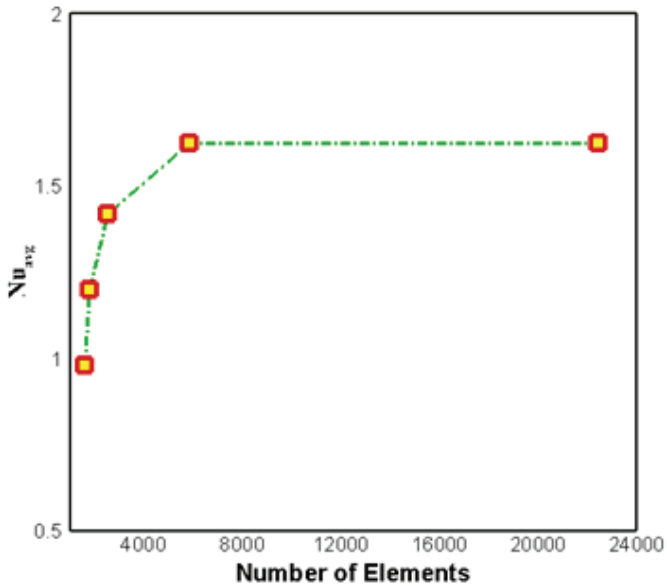

Figure 2: Mean Nusselt numbers' (Nuav) convergence for several components number when $Ra = 10^5$, $Ha = 20$, $Pr = 23.004$, $n = 3$, $\phi = 0.04$ and $\tau = 1$

contains components number such as 1589, 1782, 2530, 5820, and 22414 are scrutinized for the current wavy octagonal domain including RVW. Figure 2 shows the progress of fineness of grid which is checked by examined numerically calculating the mean Nusselt number (Nu_{av}) for the elements number hint before. A customary differentiation depicts with the mean Nusselt number values between components size 5820 and components size 22414. So, to obtain error-free results, 5820 and 22414 sized elements can easily be employed. In this research, 5820 sized component is used for having solution of grid-in-dependency and computing time limits.

Validation of Code throughout the Streamlines and the Isotherms

To acquire the definiteness of our existing numeric method, results promoted by current numeric technique has been collated with the findings of Saha et al. [40] by making use of the streamlines and the isothermal lines when $Pr = 0.71$. Figure 3 presents the differentiation of these instant results created from present numeric code with respect to the streamlines and the isotherms with formerly published research by Saha *et al.* [40]. The outcomes depict a solid authorization and magnify the credence for applying this numeric code.

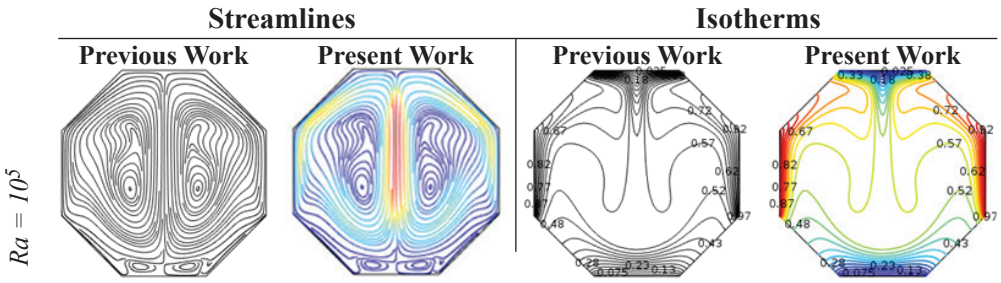

Figure 3: Collation of streamline contours and isothermal lines with Saha *et al.* [44] with current results when $Pr = 0.71$.

Outcomes and Deliberation

The calculated numeric outcomes are investigated to examine the Rayleigh numbers' ($10^3 \leq Ra \leq 10^6$) effects. The numeric calculations are expressed in terms of streamline contours, isotherm lines, velocity, temperature, regional Nusselt number and mean Nusselt number.

Solution of Evolution of Time

Figure 4 represents for Nuav, need time (τ) which is dimensionless; to reach the state in steady

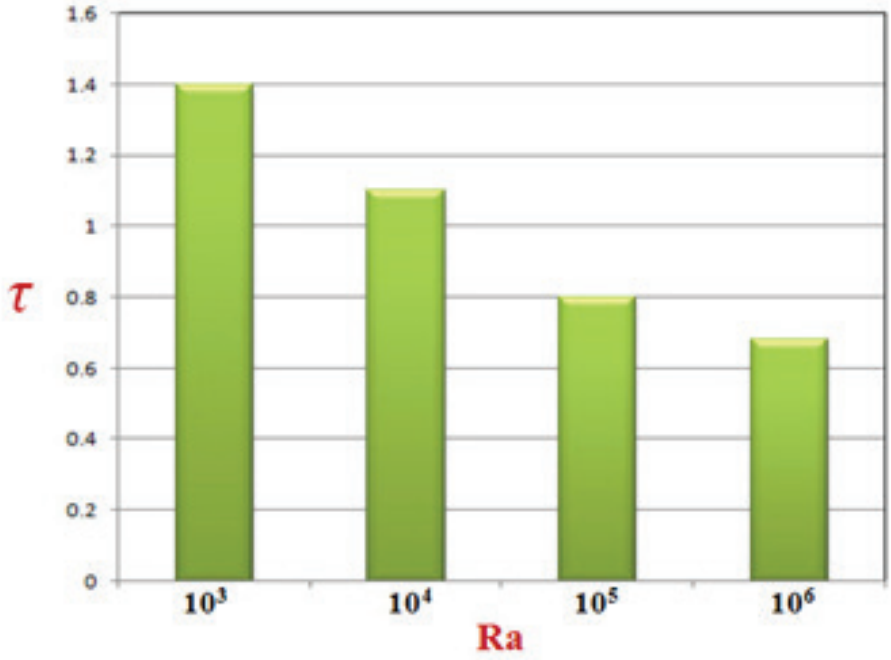

Figure 4: Non-dimensional time (τ) need the solutions for Nu_{av} to reach in steady condition for different *Ra*; Rayleigh number where ϕ = 0.04, *Ha* = 20, *Pr* = 23.004 and *n* = 3.

situation for different *Ra*; Rayleigh number where, *Pr* = 23.004, *Ha* = 20 and *n* = 3. Because of powerful buoyancy force help outs the flow to reach a steady-solution swift, in reaching from an unsteady situation to a steady condition, the flow takes less time for a higher *Ra*; Rayleigh number.

Figures 5(a) and 5(b) shows the streamlines and isothermal lines with non-dimensional time (τ) where $Ra = 10^5$, *Ha* = 20, and $\phi = 0.04$ take into consideration the step of time $\Delta\tau = 0.01$. Within immediate time, it spotted that there's two symmetric rotating

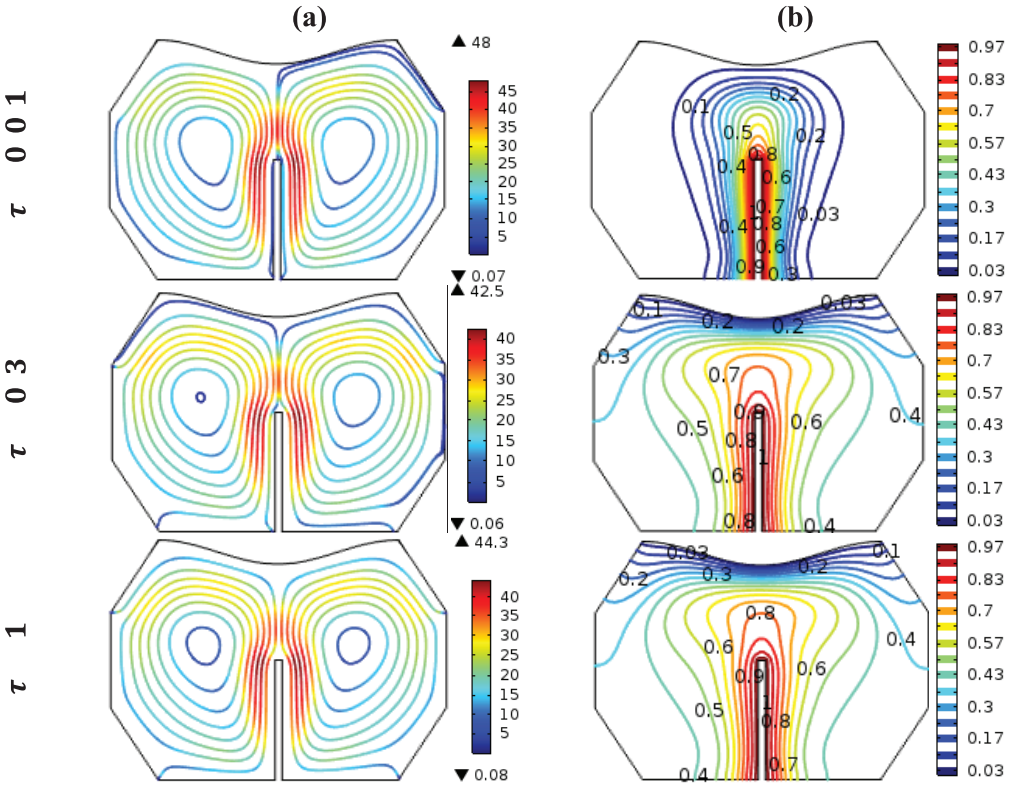

Figure 5: (a) Streamline contours and (b) isothermal lines at different non-dimensional time (τ) with $Pr = 23.004$, $Ra = 10^5$, $Ha = 20$, $n = 3$ and $\phi = 0.04$.

vortices in the domain are created in two different sides of the RVW, where near the heated RVW the origins of the rotating cells of the streamline contours are situated. Between two circulations, one is clockwise and the other is anticlockwise. The zone of rotation switched and boost up at the hot RVW and cold boundary. With intensification of time (τ) which is dimensionless, the origins of symmetric circulation become central circulation that hint an excessive velocity of flow. With the increasing value of non-dimensional time (τ), there shows no notable swaps in the streamline contours pattern until it arrive to its steady solution 5(b) plot exhibits, at τ = 0.01, flow is in unsteady-state, and isotherms are concerted near the warmed RVW border which presents elevated temperature gradient because of effects of buoyancy. As non-dimensional time (τ) grows up, the isotherms advanced upward from bottomed partition, at head of RVW, presenting giant heat flow in that area. With dimensionless time, isothermal lines' intensity grows up until

it comes to a steady-condition. Around the RVW, the isotherms shape is like a mushroom. Moreover, the isotherms commute over time and depict a minor variety till it arrive steady situation.

Effect of buoyancy force

Figures 6 represent the effects of Rayleigh number *i.e.* buoyancy force ($10^3 \leq Ra \leq 10^6$) on streamline contours for steady condition ($\tau = 1$) where $Pr = 23.004$, $\phi = 0.04$, $Ha = 20$ and $n = 3$. These results hint up that for all Ra; Rayleigh numbers, in the cavity, there's evident of buoyancy operating rotating flows.

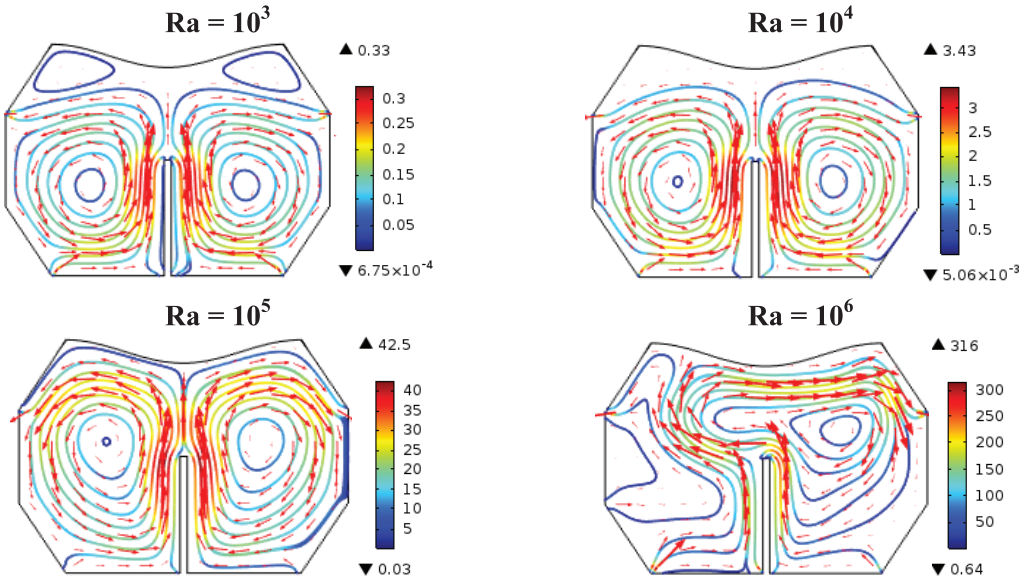

Figure 6: Effect of Ra; Rayleigh number on streamline contours for various Rayleigh number where $Ha = 20$, $n = 3$, $Pr = 23.004$, $\phi = 0.04$ and $\tau = 1$.

At steady time $\tau = 1$, for $Ra = 10^3$ two symmetric round moving cells are spotted in two sides of RVW within the enclosure. Two more vortices are observed near the wavy cold upper wall, whose are diminish for $Ra = 10^4$. The strength of rotating cells is increased for $Ra = 10^5$. All of these three figures, flow direction of one rotating cell is clockwise and the other is anticlockwise. But for $Ra = 10^6$, flow pattern changed totally. There is one rotating cell observed in the right hand side of RVW.

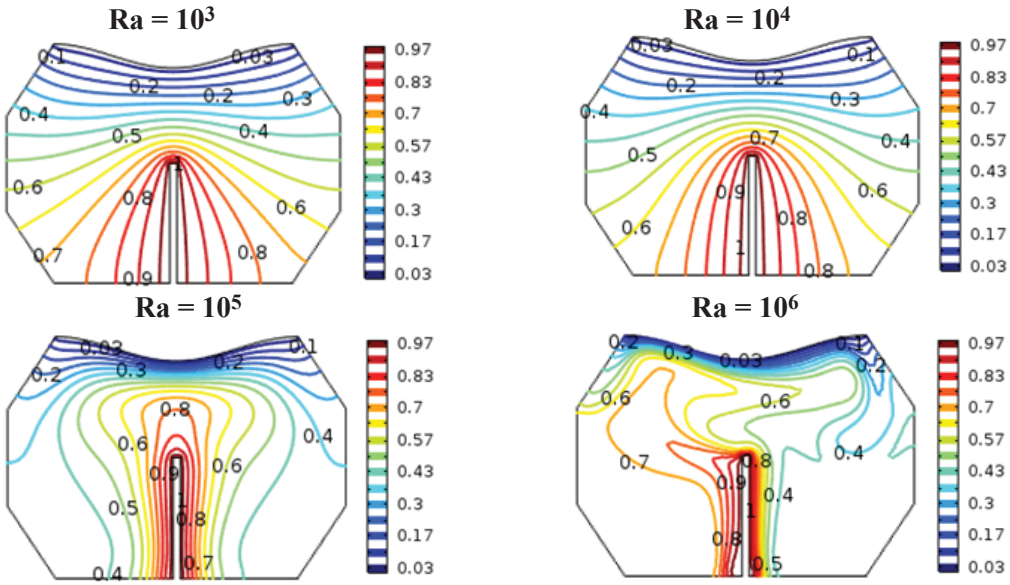

Figure 7: Effect of Rayleigh number *(Ra)* on isothermal lines for various values of Rayleigh number when $\phi = 0.04$, $Ha = 20$, $n = 3$, $Pr = 23.004$ and $\tau = 1$.

Figures 7 presents effects of the force named buoyancy *i.e.* Rayleigh number ($10^3 \leq Ra \leq 10^6$) on isotherms for steady state ($\tau = 1$) when $Pr = 23.004$, $\phi = 0.04$, $Ha = 20$ and $n = 3$. At $Ra = 10^3$; small Rayleigh number, style of isotherms is totally bend around the RVW and slowly they almost become parallel to one and all to the wavy cold boundary inside the domain for the infirm convection. The isothermal lines pattern become like parabola near the warmed RVW fence and isothermal lines are nearly parallel to each one neighbor cool wavy top boundry. Correspondingly, the important mood of heat transportation is conduction for the parameter which is lower-grade buoyancy-operated. With the increasing values of Ra, the Rayleigh numbers the power of the fluid currents enlarge because of the impact of buoyancy energies that enhance convective strength. For enhancement of buoyant operated parameter Ra, named the Rayleigh number, isotherms are gradually more deformed around the hot RVW, which hints up that the convection is starting to take over and within the domain convection become a dominant position of thermal transfer. At $^{Ra} = 10^5$ *i.e.* high Rayleigh number, the isotherm form a specific style like mushroom. This specific style of streamline contours hints that the energy of heat flows within the domain into the nanofluid from the warmed RVW. At 10^6 the higher *Ra*; Rayleigh number, the isothermal lines deformed from mushroom shape.

The local Nusselt number through the right boundary of RVW for various Rayleigh number with $Ha = 20$, $n = 3$, $Pr = 23.004$, $\phi = 0.04$ and $\tau = 1$ of the enclosure is depict in Figure 8. From the figure, it is noticed that for increasing values of Rayleigh number (Ra) local Nusselt number is increasing.

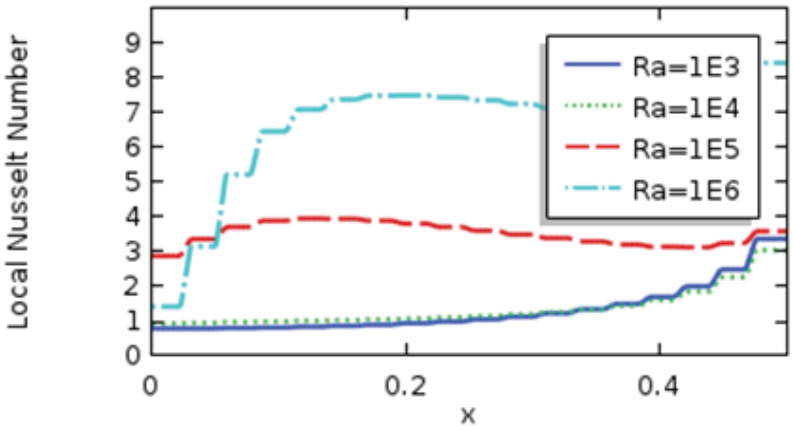

Figure 8: Local Nusselt number along right wall of hot RVW for various Rayleigh number *(Ra)* where $Ha = 20$, $Pr = 23.004$, $n = 3$, $\phi = 0.04$ and $\tau = 1$.

Terminations

The original motive of this analysis is to perform the impact of buoyancy force on MHD two-dimensional, dependent on time, incompressible, laminar flow and thermal transfer enhancement taking nanofluids inside a wavy octagonal cavity. The topper wavy border has cold at lower temperature, where the RVW on the middle of the bottom wall is warmed at higher temperature. The results for *Ra*, the Rayleigh number, have been displayed using streamline contours, isothermal lines, local Nusselt number and the mean of rate of heat transportation. From the physical point of view an extensive deliberation of these physical parameters has been done here. The significant outcomes are pointed as bellow:

- There are a significant influence in controlling the fluid flow and heat transfer for the changing of Rayleigh number (Ra)
- The heat transfer technique of the solution reaches to steady state within a very sorter time. It has been calculated approximately after $\tau = 0.68$.
- Higher Rayleigh number (Ra) conform better heat transport through convection. Heat transfer rate increase 30.33% when Ra varies 105 to 106 for kerosene-TiO_2 nanofluid.

References

1. Al-weheibi, S. M., Rahman, M. M., Alam, M. S., and Vajravelu, K., "Numerical simulation of natural convection heat transfer in a trapezoidal enclosure filled with nanoparticles," International Journal of Mechanical Sciences, vol. 131-132, pp. 599-612, 2017.

2. Balushi, L. M. A., Uddin, M. J., and Rahman, M. M., "Natural convective heat transfer in a square enclosure utilizing magnetic nanoparticles," *Propulsion and Power Research*, vol. 8(3), pp. 194-209, 2019.

3. Choi, S. U. S., and Eastman, J. A., "Enhancing thermal conductivity of fluids with nanoparticles," *Int. Mech. Eng. Cong. and Expo.*, ASME, San Francisco, USA, 1995.

4. Dogonchi, A. S., Ismael, M. A., Chamkha, A. J., and Ganji, D. D., "Numerical analysis of natural convection of Cu–water nanofluid filling triangular cavity with semicircular bottom wall," Journal of Thermal Analysis and Calorimetry, vol. 135, pp. 3485–3497, 2019.

5. Ece, M. C., and Buyuk, E., "Natural convection flow under a magnetic field in an inclined rectangular enclosure heated and cooled on adjacent wall," *Fluid Dynamics Res.*, vol. 38, pp. 564–590, 2005.

6. Ghasemi, B., Aminossadati, S. M., and Raisi, A., "Magnetic field effects on natural convection in a nanofluid-filled square enclosure," International Journal Thermal Science, vol. 50, pp. 1748-1756, 2011.

7. Hamilton, R. L., and Crosser, O. K., "Thermal conductivity of heterogeneous two-component systems," *Ind. Eng. Chem. Fundam.*, vol. 1, pp. 18-191, 1962.

8. Hwang, K., Lee, J., and Jang, J., "Buoyancy-driven heat transfer of water-based Al2O3 nanofluids in a rectangular cavity," *Int. J. Heat Mass Transf.*, vol. 50, pp. 4003–4010, 2007.

9. Jang, S. P., and Choi, S. U. S., "Role of Brownian Motion in the Enhanced Thermal Conductivity of Nanofluids," Applied Physics Letters, vol. 84(21), pp. 4316- 4318, 2004.

10. Kalbani, A. K. S., and Rahman, M. M., "Convective heat transfer in nanofluids inside an inclined square enclosure in the presence of heat source Brownian motion and oriented magnetic field," J. of Engg. Physics and Thermophysics, vol. 92(5), pp. 2188-2207, 2019.

11. Md-Fayz, A. A., Hossain, M. A., and Sarker M. M. A., "Numerical investigation of MHD mixed convection heat transfer having vertical fin in a lid-driven square cavity," AIP Conference Proceedings 2121, 030023, 2019.

12. Nasrin, R., and Parvin, S., "Investigation of buoyancy-driven flow and heat transfer in a trapezoidal cavity filled with water-Cu nanofluid," *International Communication in heat and Mass transfer*, vol. 39, pp. 270-274, 2012.

13. Oztop, H., and Abu-Nada E., "Numerical study of natural convection in partially heated rectangular enclosures filled with nanofluids," *Int. J. Heat Fluid Flow*, vol. 29, pp. 1326–1336, 2008.

14. Parvin, S., and Nasrin, R., "Effects of Reynolds and Prandtl number on mixed convection in an octagonal channel with a heat-generating hollow cylinder," Journal of Scientific Research, vol. 4(2), pp. 337-348, 2012.

15. Rahman, M. M., Mojumder, S., Saha S., Joarder A. H., Saidur R. and Naim A. G., "Numerical and statistical analysis on unsteady magnetohydrodynamic convection in a semi-circular enclosure filled with ferrofluid," International Journal of Heat and Mass Transfer,Vol. 89, pp. 1316-1330, 2015.

16. Saha, G., Saha, S., Hasan, M. N., and Islam, Md. Q., "Natural convection heat transfer within octagonal enclosure," IJE Transactions A: Basics, vol. 23(1), pp. 1-10, 2010.

17. Tinni, S., Tarikul I., Sabina Y., and Parveen, N., "Thermal influence of heated fin on MHD natural convection flow of nanofluids inside a wavy square cavity," International Journal of Thermofluids, vol. 18, Article ID 100338, 2023.

18. Uddin, M. J., and Rahman, M. M., "Finite element computational procedure for convective flow of nanofluids in an annulus," Thermal Science and Engineering Progress, Vol. 6, pp. 251-267, 2018.

19. Wong, K.V., and Leon, O. D., "Applications of nanofluids: current and future- A review article," *Advances in Mechanical Engineering*, vol. 2010, Article ID 519659, 2010.

20. Zienkiewicz, O. C., and Taylor, R. L., "The finite element method solid and structural mechanics," *Sixth Edition, McGraw-Hill*, 2005.

21. Tinni, S., Tarikul I., Sabina Y., and Parveen, N., "Thermal influence of heated fin on MHD natural convection flow of nanofluids inside a wavy square cavity," International Journal of Thermofluids, vol. 18, Article ID 100338, 2023.

22. Uddin, M. J., and Rahman, M. M., "Finite element computational procedure for convective flow of nanofluids in an annulus," Thermal Science and Engineering Progress, Vol. 6, pp. 251-267, 2018.

23. Uddin, M. J., and Rahman, M. M., "Numerical computation of natural convective heat transport within nanofluids filled semi-circular shaped enclose using nonhomogenous dynamic model," *Tharmal Science and Engineering Progress*, vol. 1, pp. 25-38, 2017.

24. Wong, K.V., and Leon, O. D., "Applications of nanofluids: current and future- A review article," *Advances in Mechanical Engineering*, vol. 2010, Article ID 519659, 2010.

25. Zienkiewicz, O. C., and Taylor, R. L., "The finite element method solid and structural mechanics," *Sixth Edition, McGraw-Hill*, 2005.